

# A NOVEL 4D PDE-BASED APPROACH FOR ACCURATE ASSESSMENT OF MYOCARDIUM FUNCTION USING CINE CARDIAC MAGNETIC RESONANCE IMAGES

Hisham Sliman<sup>1,3,\*</sup>, Ahmed Elnakib<sup>1,\*</sup>, Garth M. Beache<sup>2</sup>, Ahmed Soliman<sup>1</sup>, Fahmi Khalifa<sup>1</sup>, Georgy Gimel'farb<sup>4</sup>, Adel Elmaghraby<sup>3</sup>, and Ayman El-Baz<sup>1,†</sup>

<sup>1</sup>BioImaging Laboratory, Bioengineering Department, University of Louisville, Louisville, KY, USA.

<sup>2</sup>Department of Radiology, School of Medicine, University of Louisville, Louisville, KY, USA.

<sup>3</sup>Department of Computer Engineering and Computer Science, University of Louisville, Louisville, KY, USA.

<sup>4</sup>Department of Computer Science, University of Auckland, Auckland, New Zealand.

## ABSTRACT

A novel framework for assessing wall thickening from 4D cine cardiac magnetic resonance imaging (CMRI) is proposed. The proposed approach is primarily based on using geometrical features to track the left ventricle (LV) wall during the cardiac cycle. The 4D tracking approach consists of the following two main steps: (i) Initially, the surface points on the LV wall are tracked by solving a 3D Laplace equation between two successive LV surfaces; and (ii) Secondly, the locations of the tracked LV surface points are iteratively adjusted through an energy minimization cost function using a generalized Gauss-Markov random field (GGMRF) image model in order to remove inconsistencies and preserve the anatomy of the heart wall during the tracking process. Then the myocardial wall thickening is estimated by co-allocation of the corresponding points, or matches between the endocardium and epicardium surfaces of the LV wall using the solution of the 3D Laplace equation. Experimental results on *in vivo* data confirm the accuracy and robustness of our method. Moreover, the comparison results demonstrate that our approach outperforms 2D wall thickening estimation approaches.

**Index Terms**— Thickness, Thickening, Tracking, Cine, Cardiac, MRI

## 1. INTRODUCTION

Quantification of cardiac performance is crucial for the diagnosis and management of patients with cardiac diseases [1–4]. A number of important indicators have been employed for quantifying the cardiac performance, e.g., wall thickness, wall thickening, and functional strain [5–8]. Next, we will overview the current methods for estimating the wall thickening as well as their limitations.

**Wall Thickness Analysis:** Wall thickening is an important indicator for myocardium dysfunction, which is more accu-

rate than wall motion analysis [9–12]. It is typically assessed by visual inspection, which is preferred clinically for practical purposes [13]. However, this is obviously a time consuming process and is prone to considerable intra- and inter-observer variability which is a drawback [9, 14–16]. To overcome this, local myocardial wall thickness is derived, automatically or semiautomatically, after tracing the endocardial and epicardial boundaries in all short-axis images. Prasad et al. [17] proposed to measure the myocardial thickening in CMRI more reliably by solving a partial differential Laplace equation. However, to reduce the effects of segmentation errors in the wall thickness estimation, a further step of manual adjustment was performed by a clinical expert. Recently, Khalifa et al. [18] proposed an automated framework for analyzing the wall thickness and thickening function by solving the 2D Laplace equation. However, their method is based on 2D analysis and did not take into account the 3D motion of the cardiac wall (i.e., out-of-plane motion). Therefore, there is a need for developing more methods for more accurate wall thickness analysis.

**Limitations of Existing Works:** In summary, the above-mentioned frameworks for analyzing the regional function (i.e., wall thickening) are not sufficiently accurate and reliable for several reasons: (i) visual inspection is obviously a time consuming process and is prone to considerable intra- and inter-observer variability, and (ii) current 2D methods for wall thickening estimation lead to inaccurate measurements because they do not take into account the 3D motion of the heart (i.e., out-of-plane motion).

To overcome the aforementioned limitations, we propose a novel PDE-based method to estimate the strain and wall thickening from 4D cine CMRI based on tracking the LV wall geometry. To achieve this goal, we develop a 4D (3D+time) approach to track the LV wall points based on solving the 3D Laplace equation between each two successive surfaces over the cardiac cycle. To preserve the anatomy of the heart wall, the initially tracked surface points are iteratively refined through an energy minimization cost function using a generalized Gauss-Markov random field (GGMRF) image model.

\*Astrex indicates equal contribution

† Corresponding Author:- Tel: (502) 852-5092, Fax: (502) 852-6806, E-mail: aselba01@louisville.edu

Since we use the same image modality (i.e., cine CMRI) to estimate both wall thickening and functional strains, more correlated and accurate indexes can be obtained, which have the ability to quantify meaningful effects in treatment and physiological studies.

## 2. METHODS

The proposed framework for estimating different performance indexes of the heart (e.g., functional strain and wall thickening) from cine CMRI is schematized in Fig. 2. The segmentation of the LV wall borders can be obtained using any segmentation technique, e.g., using the method in [18] (more about segmentation methods can be found in [19]). In this paper, we focus on the tracking of the LV wall points and the assessment of the myocardial function. Details of the proposed framework are described below.

### 2.1. 4D Tracking of the LV Wall Points

**Initial tracking using the solution of the 3D Laplace equation:** In order to estimate the heart performance indexes, the surface points of the myocardium should be tracked over the cardiac cycle. In this work, we propose a geometrically motivated approach to track the surface points on the LV wall through the cardiac cycle. Our method tracks the LV surfaces' points by solving the Laplace equation between each two successive surfaces [20–23] (we denote one as the reference surface and the other one as the target surface). The Laplace equation is a second-order linear PDE:

$$\nabla^2 \Psi = \frac{\partial^2 \Psi}{\partial x^2} + \frac{\partial^2 \Psi}{\partial y^2} + \frac{\partial^2 \Psi}{\partial z^2} = 0 \quad (1)$$

where  $\Psi(x, y, z)$  is the estimated electric field between the surfaces. The solution  $\Psi$  between two surfaces results in intermediate equipotential surfaces and streamlines (field lines), being everywhere orthogonal to all equipotential surfaces and establishing natural voxel-to-voxel correspondences between the surfaces. In order to estimate  $\Psi(x, y, z)$ , we used a second order central differences method and the iterative Jacobi approach:

$$\begin{aligned} \Psi^{i+1}(x, y, z) = & \frac{1}{6} \left\{ \Psi^i(x + \theta_x, y, z) + \Psi^i(x - \theta_x, y, z) \right. \\ & + \Psi^i(x, y + \theta_y, z) + \Psi^i(x, y - \theta_y, z) \\ & \left. + \Psi^i(x, y, z + \theta_z) + \Psi^i(x, y, z - \theta_z) \right\} \quad (2) \end{aligned}$$

where  $\Psi^i(x, y, z)$  is the estimated electric field at  $(x, y, z)$  during the  $i^{th}$  iteration; and  $\theta_x, \theta_y$ , and  $\theta_z$  are the step length or resolution in  $x, y$  and  $z$  directions, respectively. Basic steps of the proposed Laplace-based tracking methodology are summarized in Algorithm 1.

---

### Algorithm 1 Solution of the 3D Laplace Equation Between Two Surfaces

---

- 1 Find the 3D edges of both LV wall surfaces.
  - 2 **Initial condition:** Set the maximum and minimum potential  $\Psi$  at the target and reference surfaces, respectively.
  - 3 Estimate  $\Psi$  between both surfaces using Eq. (2).
  - 4 Iterate Step 3 until convergence is achieved (i.e., there is no change in  $\Psi$  values between two sequential iterations).
- 

**GGMRF-based refinement:** In order to avoid any anatomical distortions that result from solving the Laplace equation, we employ a smoothness constraint to preserve the LV wall anatomy. The introduced constraint preserves the relative position between the neighboring voxels on the target LV wall surface through iterative energy minimization using a modified GGMRF image model [24] on the initially tracked points. Each tracked point on the target is iteratively refined by this model using the voxels neighborhood system ( $N$ -nearest neighbors, Fig. 2).

Given the  $N$ -nearest neighbors of each point on the target surface, the location of each point is refined using its maximum A posteriori (MAP) estimates and voxel-wise stochastic relaxation (iterative conditional mode (ICM) [25]) that jointly optimize  $x, y$ , and  $z$  spatial coordinates using [18, 26]:

$$\begin{aligned} \widehat{\mathbf{p}}_s = \arg \min_{\widetilde{\mathbf{p}}_s = (\widetilde{x}_s, \widetilde{y}_s, \widetilde{z}_s)} & \left\{ |\mathbf{x}_s - \widetilde{\mathbf{x}}_s|^\alpha \right. \\ & + \rho^\alpha \lambda^\beta \sum_{r \in N} \eta_{s,r} |\widetilde{\mathbf{x}}_s - \mathbf{x}_r|^\beta + |\mathbf{y}_s - \widetilde{\mathbf{y}}_s|^\alpha \\ & + \rho^\alpha \lambda^\beta \sum_{r \in N} \eta_{s,r} |\widetilde{\mathbf{y}}_s - \mathbf{y}_r|^\beta + |\mathbf{z}_s - \widetilde{\mathbf{z}}_s|^\alpha \\ & \left. + \rho^\alpha \lambda^\beta \sum_{r \in N} \eta_{s,r} |\widetilde{\mathbf{z}}_s - \mathbf{z}_r|^\beta \right\} \quad (3) \end{aligned}$$

where  $\mathbf{p}_s = (\mathbf{x}_s, \mathbf{y}_s, \mathbf{z}_s)$  and  $\widetilde{\mathbf{p}}_s = (\widetilde{x}_s, \widetilde{y}_s, \widetilde{z}_s)$  denote the tracked points' original locations and their expected estimates;  $N$  is the number of nearest neighbors (Fig. 2);  $\eta_{s,r}$  is the GGMRF potential, and  $\rho$  and  $\lambda$  are scaling factors. In addition to  $N$ , the parameter  $\beta \in [1.01, 2.0]$  controls the refinement level (e.g.,  $\beta = 2$  for smooth vs.  $\beta = 1.01$  for relatively abrupt edges). The parameter  $\alpha \in \{1, 2\}$  determines the Gaussian,  $\alpha = 2$ , or Laplace,  $\alpha = 1$ , prior distribution of the estimator. Our experiments below were conducted with  $\rho = 1, \lambda = 5, \beta = 1.01, \alpha = 2$ , and  $\eta_{s,r} = \sqrt{2}$  for all directions.

### 2.2. Assessment using Wall Thickness Analysis

The estimation of the wall thickening, i.e., the changes in the wall thickness during systole of the cardiac cycle, is obtained by accurate co-allocation of the corresponding points, or matches, between the inner and outer surfaces of the LV wall by solving the 3D Laplace equation. We use the geodesic distances between corresponding points to estimate the wall

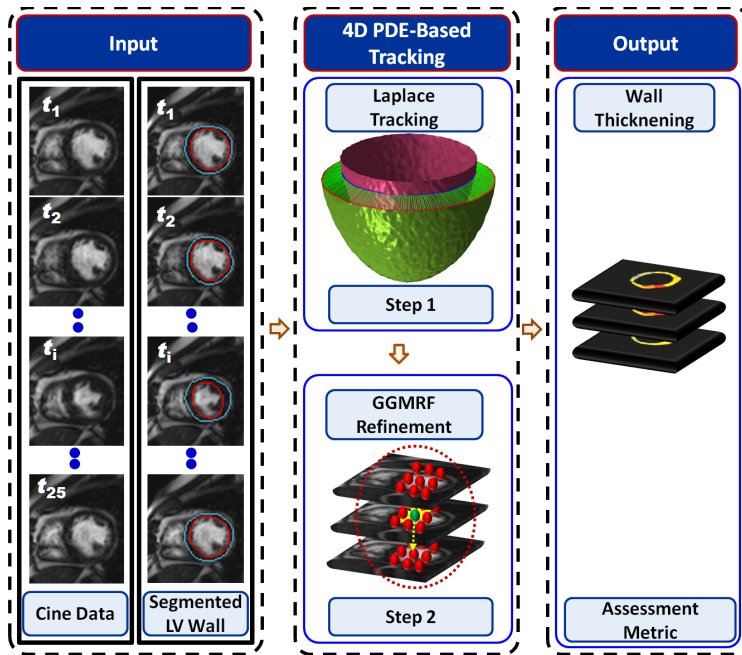


**Fig. 1.** The proposed framework for estimating the performance indexes of the heart using cine CMRI.

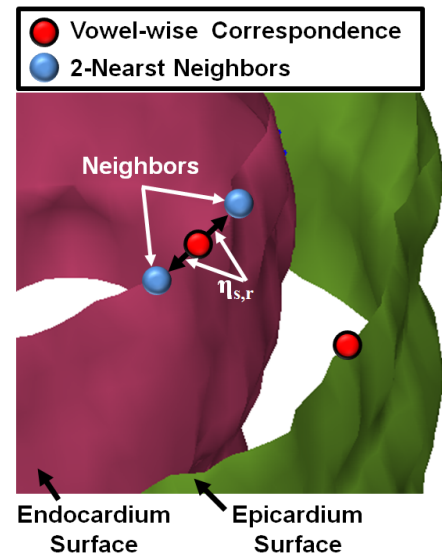


**Fig. 2.** Schematic illustration of the 2-nearest voxels.

thickness and thickening. A typical example of finding the point-wise correspondences between the inner and outer surfaces of the heart wall using the solution of the 3D Laplace equation is shown in Fig. 3.

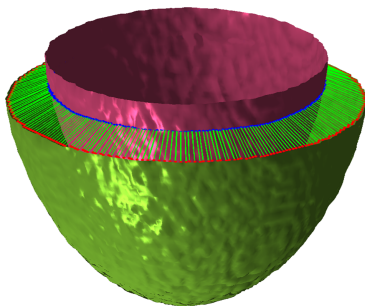


**Fig. 3.** Collocation of corresponding LV wall points for a patient data using the proposed method. The inner and outer LV wall surfaces are shown in pink and green respectively.

### 3. EXPERIMENTAL RESULTS

The proposed framework has been tested on 15 independent cine CMR data sets collected from six infarction patients who undergo a stem-cell myoregeneration therapy. Short-axis images were obtained using a 1.5 T Espree system, Siemens Medical Solutions, USA Inc., with phased array wrap-around reception coils. Breath-hold cine imaging was done using segmented True-FISP contrast. Typical parameters were: TR: 4.16 ms; TE: 1.5 ms; flip angle:  $80^\circ$ , 1 average; k-space lines

per segment: 12; isotropic in plane resolution:  $1 \times 1 \text{ mm}^2$ ; and slice thickness: 1 mm. Typically, 25 temporal image frames were obtained for each slice.

**In vivo Validation:** In order to validate our method, we compare the estimated values of the wall thickening to the ground truth (GT) values, which were estimated using a set of landmark points that were traced by a radiologist throughout the cardiac cycle. Comparison results between our method and the GT for estimating wall thickening are presented in Table 1. As demonstrated, our estimation is close to the GT as documented by the statistical paired  $t$ -test with  $P$  value greater than 0.05, which indicates non-significant difference.

To highlight the advantage of the proposed 3D method for estimating the wall thickening, we compare our method with the 2D method proposed by Khalifa et al. [18]. Unlike our method, the 2D analysis [18] shows a significant difference from the GT (the paired  $t$ -test  $P$ -value is less than 0.05, see Table 1). This is due to the fact that 2D methods do not take into account the 3D heart motion (e.g., out-of-plane motion). So our method can provide more accurate results. These results highlight the advantages of the proposed framework.

**Clinical Applications:** To emphasize the potential of using the wall thickening to document changes with treatment, we have tested our method in research participants with chronic ischemic heart disease and heart damage who underwent a stem-cell myoregeneration therapy. For visual assessment of the wall thickening ( $\delta$ ) functional parameter, we use a voxel-wise parametric (color-coded) map. To derive these functional maps, each  $\delta$  value is normalized by relating it to the

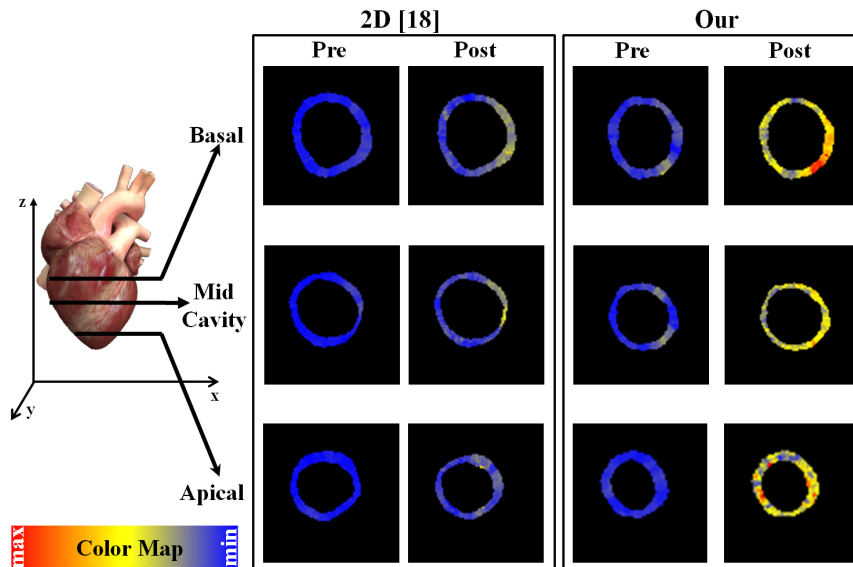


**Fig. 4.** Pre- and post-thickening analysis using the 2D method proposed in [18] and our proposed method for a patient enrolled in this study. The results are projected on 2D basal, mid-cavity, and apical cross-sections for illustration.

**Table 1.** Comparison results for mean thickening and over the cardiac cycle using our method versus the ground truth, estimated using 12 selected landmarks. Our thickening analysis is compared to the 2D thickening analysis proposed in [18].

	Metric 1: Wall Thickening		<i>P</i> -value
	Mean	Standard Deviation	
GT	5.74 mm	2.24 mm	
Our	5.66 mm	1.94 mm	0.9439
2D [18]	1.42 mm	0.98 mm	0.0005

maximum value measured in the whole volume for the pre- or post-treatments, for the given subject. Fig. 4 and Fig. 5 present the parametric maps for the  $\delta$  values over multiple cross-sections for pre- and post-therapy of two subjects. As shown in Fig. 4, our 4D method can better detect the variability of the wall thickening than the 2D method proposed by Khalifa et al. [18]. These results emphasize the potential of using the wall thickening to document changes with treatment that were consistent with improvements in patient condition, as documented by clinical indexes. This lends encouragement for the proposed framework to detect and quantify meaningful effects in treatment and physiological studies.

#### 4. CONCLUSIONS

A novel 4D (3D+time) tracking approach for accurate assessment of myocardium function using cine CMRI is presented. The experimental results on *in vivo* data demonstrated the ability of the proposed approach for detecting the out-of-plane heart motion which leads to accurate estimation of 4D wall thickening assessment metric. The main advantage of

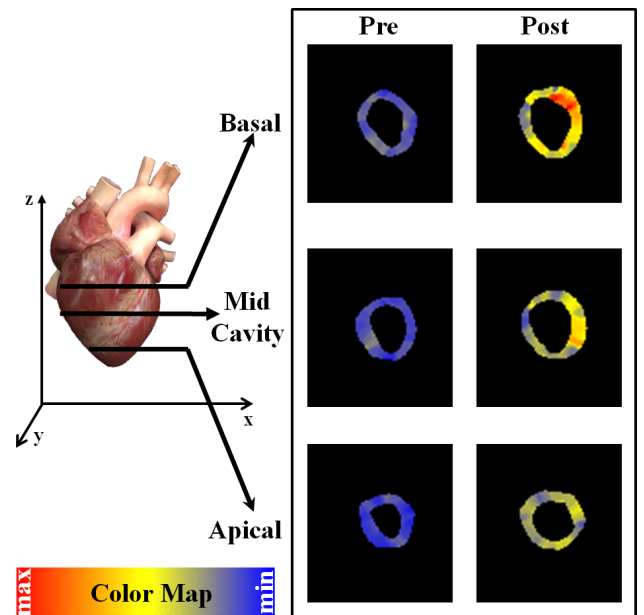


**Fig. 5.** Pre- and post-thickening analysis for another patient enrolled in this study, projected on 2D basal, mid-cavity, and apical cross-sections for illustration.

4D regional analysis using cine CMRI is that it allows better detection of the variability of the wall thickening than the 2D methods. In the future, we plan to estimate and correlate other global (e.g., ejection fraction) and local (e.g., functional strain) assessment metrics, derived from cine CMRI, for patients enrolled in our case study, stem-cell myoregeneration therapy.

## 5. REFERENCES

- [1] M. Y. Henein (Editor), *Heart failure in clinical practice*, Springer-Verlag: London, 2010.
- [2] M. Nitzken, G. Beache, A. Elnakib, F. Khalifa, G. Gimel'farb, and A. El-Baz, "Improving full-cardiac cycle strain estimation from tagged CMR by accurate modeling of 3D image appearance characteristics," *Proc. IEEE International Symposium on Biomedical Imaging: From Nano to Macro (ISBI'12)*, Barcelona, Spain, May 2–5, 2012, pp. 462–465.
- [3] H. Sliman, F. Khalifa, A. Elnakib, A. Soliman, G. M. Beache, A. Elmaghraby, and A. El-Baz, "A new segmentation-based tracking framework for extracting the left ventricle cavity from cine cardiac MRI," *Proc. IEEE International Conference Image Processing (ICIP'13)*, Melbourne, Australia, September 15–18, 2013, pp. 685–689.
- [4] H. Sliman, F. Khalifa, A. Elnakib, A. Soliman, A. El-Baz, G. M. Beache, A. Elmaghraby, and G. Gimel'farb, "Myocardial borders segmentation from cine MR images using bidirectional coupled parametric deformable models," *Medical Physics*, vol. 40, no. 9, 2013.
- [5] G. M. Beache, V. Wedeen, and R. Dinsmore, "Magnetic resonance imaging evaluation of left ventricular dimensions and function and pericardial and myocardial disease," *Coronary Artery Disease*, vol. 4, no. 4, pp. 328–333, 1993.
- [6] M. Nitzken, G. Beache, A. Elnakib, F. Khalifa, G. Gimel'farb, and A. El-Baz, "Accurate modeling of tagged CMR 3D image appearance characteristics to improve cardiac cycle strain estimation," *Proc. IEEE International Conference on Image Processing (ICIP'12)*, Orlando, Florida, USA, September 30–October 3, 2012, 521–524.
- [7] A. Elnakib, G. M. Beache, H. Sliman, G. Gimel'farb, T. Inanc, and A. El-Baz, "A novel laplace-based method to estimate the strain from cine cardiac magnetic resonance images," *Proc. IEEE International Conference Image Processing (ICIP'13)*, Melbourne, Australia, September 15–18, 2013, pp. 690–694.
- [8] A. Elnakib, G. M. Beache, G. Gimel'farb, T. Inanc, and A. El-Baz, "Validating a new methodology for strain estimation from cardiac cine MRI," *Proc. Int. Symp. Computational Models for Life Sciences*, Sydney, Australia, November 27–29, vol. 1559, no. 1, pp. 277–286, 2013.
- [9] E. R. Holman, H. W. Vliegen, R. J. van der Geest, J. H. C. Reiber, P. R. van Dijkman, A. van der Laarse, A. de Roos, and E. E. van der Wall, "Quantitative analysis of regional left ventricular function after myocardial infarction in the pig assessed with cine magnetic resonance imaging," *Magnetic Resonance in Medicine*, vol. 34, no. 2, pp. 161–169, 1995.
- [10] S. Sasayama, D. Franklin, J. Ross Jr, W. S. Kemper, and D. McKown, "Dynamic changes in left ventricular wall thickness and their use in analyzing cardiac function in the conscious dog: A study based on a modified ultrasonic technique," *The American Journal of Cardiology*, vol. 38, pp. 870–879, 1976.
- [11] F. H. Sheehan, E. L. Bolson, H. T. Dodge, D. G. Mathey, J. Schofer, and H. W. Woo, "Advantages and applications of the centerline method for characterizing regional ventricular function," *Circulation*, vol. 74, pp. 293–305, 1986.
- [12] H. Azhari, S. Sideman, J. L. Weiss, E. P. Shapiro, M. L. Weisfeldt, W. L. Graves, W. J. Rogers, and R. Beyar. "Three-dimensional mapping of acute ischemic regions using MRI: Wall thickening versus motion analysis," *Am J Physiol*, vol. 259, no. 5, pp. H1492–H1503, 1990.
- [13] S. Pujadas, G. P. Reddy, O. Weber, J. J. Lee, C. B. Higgins, "MR Imaging Assessment of Cardiac Function," *Journal of Magnetic Resonance Imaging*, vol. 19, pp. 789–799, 2004.
- [14] C. D. von Land, S. R. Rao, and J. H. C. Reiber, "Development of an improved centerline wall motion model," *IEEE Proceedings of Computers in Cardiology*, pp. 687–690, 1990.
- [15] R. J. van der Geest, A. de Roos, E. E. van der Wall, J. H. C. Reiber, "Quantitative analysis of cardiovascular MR images," *Int J Card Imaging*, vol. 13, pp. 247–258, 1997.
- [16] N. Beohar, J. D. Flaherty, C. J. Davidson, M. I. Vidovich, A. Brodsky, D. C. Lee, E. Wu, E. L. Bolson, R. O. Bonow, and F. H. Sheehan, "Quantitative assessment of regional left ventricular function with cardiac MRI: Threedimensional centersurface method," *Catheterization Cardiovasc. Interv.*, vol. 69, no. 5, pp. 721–728, 2007.
- [17] M. Prasad, A. Ramesh, P. Kavanagh, J. Gerlach, G. Germano, D. S. Berman, and P. J. Slomka, "Myocardial wall thickening from gated magnetic resonance images using Laplaces equation," in *Proc. SPIE2009*, 2009, vol. 72602I, pp. 18.
- [18] F. Khalifa, G. M. Beache, G. Gimel'farb, G. A. Giridharan, and A. El-Baz, "Accurate Automatic Analysis of Cardiac Cine Images," *IEEE Trans. Biomedical Engineering*, vol. 59, 2012.
- [19] A. Elnakib, G. Gimel'farb, J. S. Suri, and A. El-Baz, "Medical image segmentation: A brief survey," In *Multi Modality State-of-the-Art Medical Image Segmentation and Registration Methodologies, Volume 2*, (A. El-Baz, R. Acharya, A. Laine, and J. Suri, Editors), Springer, New York, 2011, pp. 1–39.
- [20] F. Khalifa, A. El-Baz, G. Gimel'farb, and M. Abo El-Gahr, "Non-invasive image-based approach for early detection of acute renal rejection," *Proc. of International Conference on Medical Image Computing and Computer-Assisted Intervention (MICCAI'10)*, 2010, vol. 1, pp. 10–18.
- [21] A. Elnakib, G. M. Beache, M. Nitzken, G. Gimel'farb, and A. El-Baz, "A new framework for automated identification of pathological tissues in contrast enhanced cardiac magnetic resonance images," *Proc. IEEE International Symposium on Biomedical Imaging: From Nano to Macro (ISBI'11)*, Chicago Illinois, USA, March 30–April 2, pp. 1272–1275, 2011.
- [22] A. Elnakib, G. M. Beache, G. Gimel'farb, and A. El-Baz, "New automated Markov-Gibbs random field based framework for myocardial wall viability quantification on agent enhanced cardiac magnetic resonance images," *Int J Cardiovasc Imaging*, vol. 28, no. 7, pp. 1683–1698, 2012.
- [23] F. Khalifa, M. Abou El-Ghar, B. Abdollahi, H. B. Frieboes, T. El-Diasty, and A. El-Baz, "A comprehensive non-invasive framework for automated evaluation of acute renal transplant rejection using DCE-MRI," *NMR in Biomedicine*, vol. 26, no. 11, pp. 1460–1470, 2013.
- [24] C. Bouman and K. Sauer, "A generalized Gaussian image model for edge-preserving MAP estimation," *IEEE Trans. Medical Imaging*, vol. 2, no. 3, pp. 296–310, 1993.
- [25] J. Besag, "On the statistical analysis of dirty pictures," *Journal of the Royal Statistical Society. Series B*, vol. 48, no. 3, pp. 259–302, 1986.
- [26] A. El-Baz, "Novel stochastic models for medical image analysis," *PhD Thesis*, University of Louisville, Louisville, KY, USA, 2006.